

Physical realization of two-dimensional Ising critical phenomena: Oxygen chemisorbed on the W(112) surface

G.-C. Wang*

Solid State Division, Oak Ridge National Laboratory, Oak Ridge, Tennessee 37831

T.-M. Lu

*Center for Integrated Electronics and Department of Physics,
Rensselaer Polytechnic Institute, Troy, New York 12180-3590*

(Received 19 October 1984)

The continuous reversible order-disorder phase transition of oxygen chemisorbed on the W(112) surface at half-monolayer coverage was studied by low-energy electron diffraction (LEED). The critical phenomena associated with this phase transition are shown to belong to the two-dimensional Ising universality class. An attempt has been made to extract the critical exponents, and the limitations of the LEED system presently used are discussed.

Recently it has been shown that continuous order-disorder phase transitions for localized adsorption on surfaces may exhibit different universality class behavior.^{1,2} Among them, the two-dimensional (2D) Ising universality class is of particular interest. This system is perhaps the most significant nontrivial statistical problem which has been solved exactly with mathematical rigor.³ In this paper, we present an experimental study of the 2D Ising phase transition in a lattice gas system using low-energy electron diffraction (LEED). Critical behavior of other universality classes that have been studied in the area of chemisorption are the four-state Potts model, Ni(111) $p(2 \times 2)$ (Ref. 4) and the X - Y model with fourfold (cubic) anisotropy, W(110) $p(2 \times 1)$ -H and W(110) $p(2 \times 2)$ -H.⁵

Oxygen chemisorbed on a W(112) surface forms a $p(2 \times 1)$ superstructure over a wide range of submonolayer coverage at room temperature and has been observed previously by LEED.^{6,7} A representation of the adsorbed layer is shown in Fig. 1. The structures of both the clean W(112) surface and a half-monolayer (ML) oxygen-covered $p(2 \times 1)$ -O surface have been determined by a comparison between LEED experimental intensity-versus-energy (I - V) profiles and a dynamical LEED model calculation, and results show a nonreconstruction surface (or 1×1 reconstruction) and a simple overlayer, respectively.⁸

Details of the experimental setup have been described elsewhere.⁹ The W(112) was cleaned in a UHV chamber (8×10^{-11} Torr) using O_2 and heat treatments until no impurities were detected by Auger-electron spectroscopy (AES). The adsorption of high-purity oxygen (99.9999%) on the clean surface was performed at either room temperature or 170 K using a molecular jet positioned near the sample. A typical exposure required to obtain a 0.5 ML of oxygen was about 0.2 L (1×10^{-9} Torr partial pressure of oxygen for 200 s). (1 L = 1 Langmuir = 10^{-6} Torr.s.) After exposure, the overlayer was thermally annealed to 630 K and then cooled to near room tempera-

ture. This process always produced the most intense fractional order diffracted beams on a fluorescence screen or the highest intensity measured by a Faraday cup (a 0.5-mm-diameter aperture which makes an acceptance angle of 1.5° with respect to the sample surface) due to the elimination of antiphase domain boundaries.¹⁰ The heating of the surface to temperatures below 1000 K was provided by radiation heating from the back side of the crystal. The temperature readings were recorded using W(26 at.%)Re-W(5 at.%)Re thermocouple wires attached to the front side of the crystal where the electron diffraction takes place. The estimated error in absolute temperature at very high temperatures (~ 1000 K) is about ± 5 K, but the relative uncertainty in temperature is less than 2 K even at these high temperatures.

The temperature dependence of the peak intensities $I(T)$ of $(\frac{1}{2} 0)$ beams follows the Debye-Waller behavior at

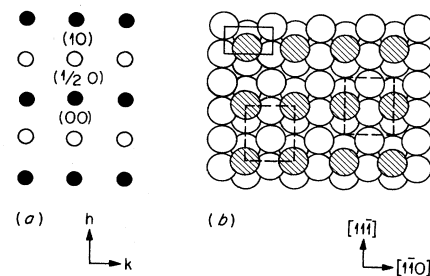


FIG. 1. (a) Schematic LEED pattern of W(112) $p(2 \times 1)$ -O at half-monolayer coverage. Solid circles, integral-order beams; open circles, half-order beams. (b) Schematic drawing of the $p(2 \times 1)$ -O layer on a W(112) surface. Open circles, W atoms; hatched circles, oxygen atoms; solid-line rectangle, $p(1 \times 1)$ substrate unit mesh; dashed-line rectangles, $p(2 \times 1)$ superlattice unit mesh. There are two possible positions of $p(2 \times 1)$ unit mesh which have antiphase relationship with respect to each other.

temperatures lower than 700 K. $I(T)$ is defined to be the intensity collected by the Faraday cup detector at the peak position of the angular distribution of the superlattice beam. For temperatures higher than 700 K, the intensity starts to deviate from the Debye-Waller slope and falls off much more rapidly.^{6,9} Figure 2 shows the normalized temperature-dependent peak intensity for both heating and cooling. Within experimental uncertainty, the process is reversible. Also shown in the same figure is the measured temperature-dependent full width at half maximum (FWHM) of the angular intensity distribution of the $(\frac{1}{2} 0)$ beam, obtained by scanning the Faraday cup across the diffracted beam in the h direction (see Fig. 1). The broadening of the FWHM away from the instrument response width indicates the disappearance of the long-range order and appearance of short-range order above a transition temperature. This broadening is an indication of a continuous phase transition. We have also measured the temperature dependence of the peak intensities and FWHM of the integral order beams from both clean and oxygen-covered surfaces. In contrast to the results obtained from the $(\frac{1}{2} 0)$ beams, the $I(T)$ always follows the Debye-Waller slope up to 1000 K, and the FWHM do not broaden.⁹ These observations indicate that the substrate tungsten provides the 2D absorption lattice sites for the oxygen overlayer. The abrupt change in intensities and FWHM of the $(\frac{1}{2} 0)$ beams is attributed to the order-disorder phase transition in the overlayer.

We have further measured the amount of oxygen adsorbed on the surface over a wide range of temperature using AES, including the temperature region where the rapid change of $(\frac{1}{2} 0)$ beam intensity occurs. The AES results show that the O/W signal ratio stays constant over the entire temperature range. Oxygen can only be desorbed at $T > 2200$ K. We therefore have a 2D "closed system."

The LEED pattern shows that the disordered phase of the oxygen overlayer is (1×1) which has a $P2mm$ space group symmetry. The order parameter ϕ_k of the ordered $p(2 \times 1)$ phase has only one component. One can obtain the Landau-Ginzburg-Wilson Hamiltonian by construct-

ing all possible invariants of the ϕ_k under all elements of $P2mm$ and the final form is identical to that of the 2D Ising Hamiltonian. The order-disorder phase transition of oxygen on the W(112) surface at a half-monolayer coverage thus belongs to the 2D Ising universality class.

The order-disorder transition at coverages other than half-monolayer have also been measured and a complete phase diagram ($T-\Theta$) has been reported previously.^{9,10} At exactly 0.5-ML coverage, the transition temperature is the highest, and this mechanism serves as the most reliable way to determine the 0.5 ML coverage. Also, this high transition temperature (~ 900 K) allows the critical region to span a much wider absolute-temperature range for the same range of reduced temperature $[|t| = |(T-T_c)/T_c|]$ as compared with other low-transition-temperature systems.^{4,5} This wide temperature range allows more data to be used for extracting critical exponents, thus producing more reliable values.

Next, we present the critical exponents extracted from the critical region (Fig. 2). The LEED intensity of a superlattice beam scattered from an adsorbed overlayer that undergoes a continuous order-disorder phase transition consists of a Bragg diffraction term which describes the temperature dependence of the square of the order parameter (long-range order) for $T < T_c$, and a diffuse scattering term describing the critical fluctuation (short-range order) near T_c .¹¹

The theory of critical phenomena predicts that in the vicinity of T_c (the critical region), the function $F(T)$ varies according to a power law,

$$F(T) = F_\lambda |T - T_c|^\lambda. \quad (1)$$

For $T < T_c$, $F(T) = I_l(T)$ and $\lambda = 2\beta$; for $T > T_c$, $F(T) = I_s(T)$ and $\lambda = -\gamma$, and $F(T) = W_s(T)$ and $\lambda = \nu$, where F_λ is a constant, β is the critical exponent associated with the long-range order (magnetization), and γ and ν are exponents associated with susceptibility and correlation length, respectively. I_l and I_s are the peak intensities due to long-range order and short-range order, respectively, and W_s is the FWHM of the short-range scattering.

The choice of the critical region will affect the resultant values of T_c and critical exponents. First we have to determine the data range to be used for fitting. We followed the method used by Lyuksyutov and Fedorus⁵ to extract β . Using Eq. (1), one plots $\ln I_l(T)$ versus $\ln(T_c - T)/T_c$ using T_c as a variable looking for a linear relationship. Using this method we deduce that the plot of experimental data is consistent with straight-line behavior in the temperature range of $T_c - 75$ K ($|t| = 0.083$) to $T_c - 15$ K ($|t| = 0.016$) for 894 K $< T_c < 904$ K (or, $T_c = 899 \pm 5$ K). The result is shown in Fig. 3.

In reality, the 2D system contains domains of finite size. This is due to the existence of imperfection of the substrate and possible "frozen-in" antiphase boundaries.^{10,12} This finite size of domains results in "smearing" of the phase transition¹³ and leaves a tail above an average T_c . In practice, we should fit Eq. (1) in a temperature region not too close to T_c . The closest value of T can be estimated as follows: It has been shown that the

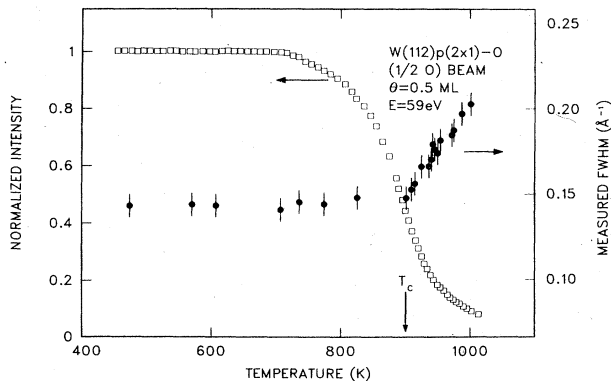


FIG. 2. Normalized peak intensity and FWHM vs temperature of a superlattice beam. Open squares, measured peak intensity corrected by Debye-Waller factor; solid circles, measured FWHM.

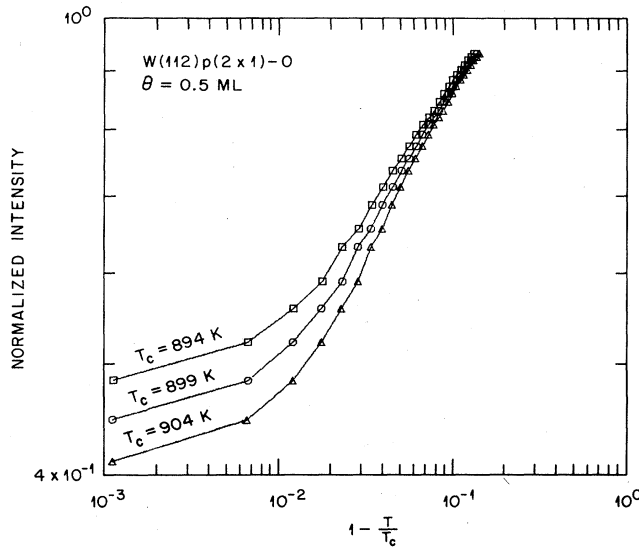


FIG. 3. Peak intensity of $(\frac{1}{2} 0)$ beam vs reduced temperature in logarithmic coordinates for $\Theta=0.5$ ML. Open squares, $T_c=894$ K; open circles, $T_c=899$ K; open triangles, $T_c=904$ K.

fluctuation correlation length r_c increases at $T \rightarrow T_c$ and obeys¹⁴ the functional relationship:

$$r_c \sim a \left(\frac{|T_c - T|}{T_c} \right)^{-\nu}, \quad (2)$$

where a is the lattice constant. For a 2D Ising class, theoretical ν equals 1, thus r_c is reduced to $a(T_c/|T_c - T|)$. The power-law behavior predicts that only for a domain size $L > r_c$ will all the quantities be observed.¹⁴ From the characterization of the surface perfection we know that there is a lower limit of detectable perfect region of $L \sim 200$ Å.⁹ Thus, if $r_c \sim 200$ Å, $a \sim 3$ Å, $T_c \sim 900$ K, we obtain $|T_c - T| \sim 13.5$ K. This value is in good agreement with the choice of critical region, as discussed above, following the method used by Lyuksyutov and Fedorus.⁵

Following Horn *et al.*¹³ we assume a finite-width Gaussian distribution of the critical temperatures Δt due to the finite-size domains and fit the measured $I_l(T)$ with the aid of the formula

$$I_c = \frac{I_0}{\sqrt{2\pi} \Delta t} \int_{T-T_c}^{\infty} \left[\frac{T_c - T + t}{T_c + t} \right]^{2\beta} \times \exp \left[-\frac{1}{2} \left(\frac{t}{\Delta t} \right)^2 \right] dt. \quad (3)$$

For $0.01 < |t| < 0.09$, i.e., $813 \pm 10 < T < 883 \pm 5$ K, the results obtained from Eq. (3) are $\beta=0.127 \pm 0.01$, $T_c=899 \pm 4$ K, $\Delta t=4 \pm 1$ K, $I_0=1.56 \pm 0.01$, $F < 1 \times 10^{-4}$, where F is the sum of the square of the difference between measured I_l and calculated I_c . The calculated $I_c(T)$ using the best fitted parameters $\beta=0.127$, $T_c=899$ K and $\Delta t=4$ K follows closely the measured I_l for $813 < T < 883$ K.

To extract critical exponent γ and ν for $T > T_c$, the measured angular profile of the $(\frac{1}{2} 0)$ beam at 59 eV, after subtraction of the diffuse background was compared with a parametrized Lorentzian function (two parameters, peak height, and FWHM) convoluted with an instrument response function which is taken from the angular profile of the $(\frac{1}{2} 0)$ beam at low temperature (~ 300 K). The process was repeated for angular profiles measured at different temperatures to extract the peak height $I_s(T)$ and FWHM(T). Four of the calculated angular profiles, using the optimum values of peak height and FWHM, are shown as solid curves in Fig. 4 and the measured data shown as circles. $S_{||}$ is the momentum transfer parallel to the surface. The temperature dependence of the inverse peak height $1/I_s(T)$, and FWHM, $W_s(T)$, are shown in Figs. 5 and 6, respectively. These data are then fitted by the power law, Eq. (1), for $T > T_c$. The fitted curves are shown as dashed lines in Figs. 5 and 6. Again, the choice of temperature range and different T_c affect the values of γ and ν . However, the effect is relatively less serious as compared with the case of extracting β . Results of the

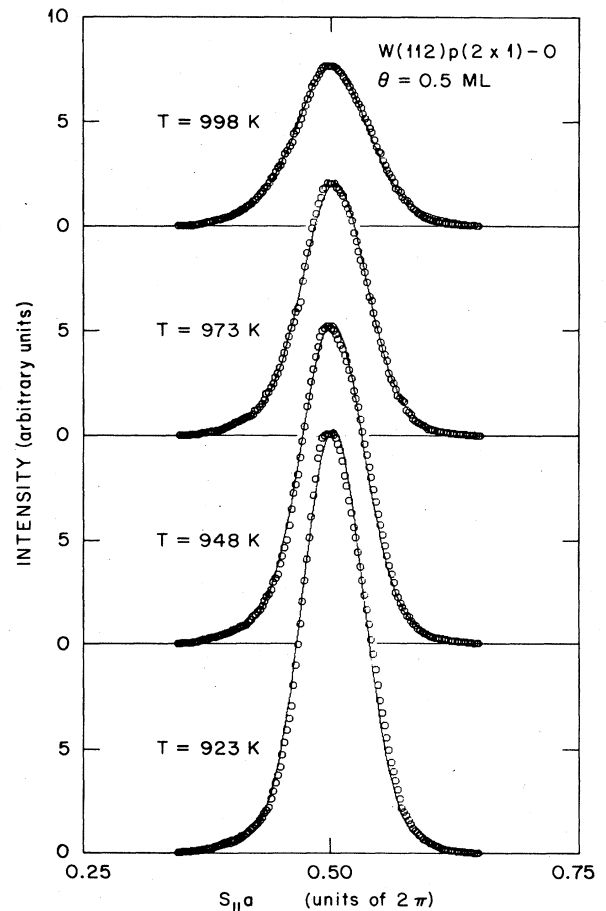


FIG. 4. Angular profiles of LEED $(\frac{1}{2} 0)$ beams for the $W(112)p(2 \times 1)-O$ system measured at $T=923, 948, 973,$ and 998 K. Open circles, experimental values; solid curves, calculated values. $S_{||}$ is the momentum transfer parallel to the surface.

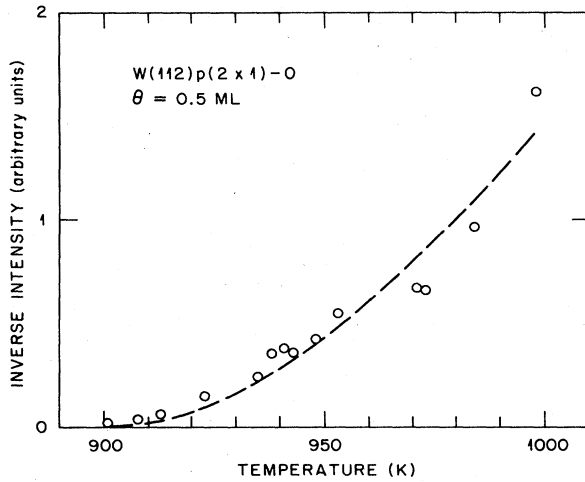


FIG. 5. Inverse peak intensity vs temperature for $T > T_c$. Dashed curve, power-law fit.

analysis are listed in Table I. If $T_c = 899$ K, the γ obtained by fitting 14 data points of $I_s(T)$ ranging from $0.002 < |t| < 0.110$ is 1.779(7); the γ obtained by fitting 12 data points of $I_s(T)$ ranging from $0.015 < |t| < 0.110$ is 1.779(2). The two γ 's differ by $< 1\%$. In the case of ν , the result obtained by fitting 14 data points of $W_s(T)$ ranging from $0.002 < |t| < 0.110$ is 1.092. If 12 data points of $W_s(T)$ ranging from $0.015 < |t| < 0.110$ were used, the ν obtained is 1.082. The two ν 's differ by $\sim 1\%$. The choice of different T_c will also affect the values of γ and ν . For example, if T_c is changed from 899 to 904 K, the γ obtained is 1.650 (7.2% change from 1.779) for $0.010 < |t| < 0.110$. If T_c is lowered from 899 to 894 K, the γ obtained is 1.947 (9.4% change from 1.779) for $0.002 < |t| < 0.110$. In the case of ν , if T_c is increased from 899 to 904 K, ν changes from 1.092 to 0.978 (10.4% change) for $0.010 < |t| < 0.110$. If T_c is decreased from 899 to 894 K, ν changes from 1.092 to 1.205 (10.4% change) for $0.002 < |t| < 0.110$. The final values determined for the critical exponents are listed in Table II. The errors associated with β , γ , and ν are the result of allowing ± 5 K change in T_c (899 K). For comparison,

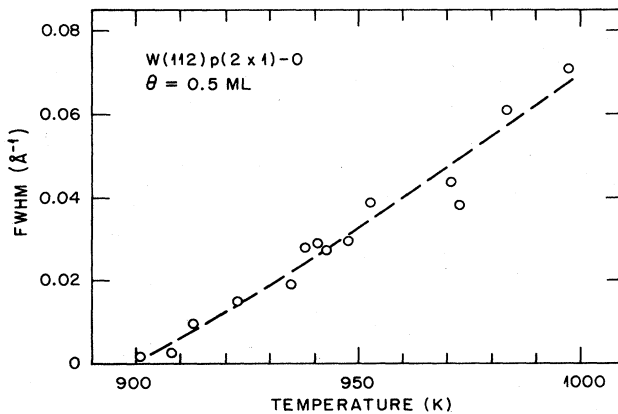


FIG. 6. FWHM vs temperature for $T > T_c$. Dashed curve, power-law fit.

TABLE I. Results of analysis.

T_c (K)	Number of points	Range of $ t $	γ	ν
899	14	0.002–0.110	1.779(7)	1.092
899	12	0.015–0.110	1.779(2)	1.082
904	14	0.010–0.110	1.650	0.978
894	14	0.002–0.110	1.947	1.205

theoretical predictions of Ising, and 3- and 4-state Potts model are also listed in Table II.

An alternative method was employed to extract γ and ν using only the peak intensity decay for $T > T_c$ instead of the entire angular profile. The normalized measured peak intensities as a function of T for $T > T_c$ were compared with the integration of the product of a parametrized Lorentzian (four parameters, C_1 , C_2 , γ , and ν) with a Gaussian instrument response function (taken at 300 K):

$$I(k_0, T)$$

$$= \int_{\pi/2a}^{3\pi/2a} T(k - k_0) \frac{C_1 |1 - (T/T_c)|^{2\nu - \gamma}}{(k - k_0)^2 + C_2 |1 - (T/T_c)|^{2\nu}} dk,$$

where $k_0 = 2\pi/2a$ is the Bragg position of a superlattice beam. The measured peak intensity $I(k_0, T)$ should contain information on both I_s and W_s because of the instrumental broadening (convolution) effect. For 903 K $< T < 993$ K, the values obtained for γ (~ 1.58 and 0.79) are within 10% and 20%, respectively, of the γ and ν obtained from the first method and are less sensitive to change of T_c and temperature range of fitting.

In principle, the critical exponents extracted from different superlattice beams should yield the same results if the temperature dependence of multiple scattering contribution^{4,11,15} is negligible. We have not performed detailed measurement and analysis of the temperature dependence of superlattice beams other than the $(\frac{1}{2}, 0)$ beam.

In summary, we have used LEED to study the order-disorder phase transition of oxygen chemisorbed on a W(112) surface at a half-monolayer coverage. We showed that this 2D lattice gas system is a physical realization of the 2D Ising universality class. The critical exponents extracted from the measurements are consistent with those expected for that class. The large error ($\sim 10\%$) introduced in the determination of the values of the exponents comes mainly from the finite-size effect and the finite instrumental resolution. With the recent development of the high-resolution LEED systems,^{16,17} which allow one to resolve a domain size of 7000–10 000 Å, one should be able to improve accuracy drastically. We also caution that the analysis in this work is based on the kinematic

TABLE II. Final values determined for the critical exponents and theoretical predictions.

Experimental	Theory		
	2D Ising	3-state Potts	4-state Potts
$\beta = 0.13 \pm 0.01$	$\frac{1}{8}$	$\frac{1}{9}$	$\frac{1}{12}$
$\gamma = 1.79 \pm 0.14$	$\frac{7}{4}$	$\frac{13}{9}$	$\frac{7}{6}$
$\nu = 1.09 \pm 0.11$	1	$\frac{5}{6}$	$\frac{2}{3}$

approximation. Although it has been argued qualitatively^{4,11,15} that multiple scattering contributions in the temperature dependence of the LEED intensity scattering from the overlayer should be small, quantitative estimation on the other hand, one should be able to test experimentally the effect of multiple scattering by measuring accurately the critical exponents for different diffraction geometry using the high-resolution LEED systems.

We thank M. G. Lagally, L. D. Roelofs, P. A. Bennett, J. C. Wang, M. Rasolt, D. M. Zehner, and S. C. Fain for invaluable discussions and suggestions. This research was sponsored by the Division of Materials Sciences, U. S. Department of Energy under contract DE-AC05-84OR21400 with Martin Marietta, Energy Systems, Inc., and the Center for Integrated Electronics, Rensselaer Polytechnic Institute.

*Present address: Department of Physics, Rensselaer Polytechnic Institute, Troy, New York, 12180-3590.

¹E. Domany, M. Schick, J. S. Walker, and R. B. Griffiths, *Phys. Rev. B* **18**, 2209 (1978); **20**, 3828 (1979).

²C. Rottman, *Phys. Rev. B* **24**, 1482 (1981); I. P. Ipatova, Yu. E. Kitaev, and A. V. Subashiev, *Surf. Sci.* **110**, 543 (1981).

³L. Onsager, *Phys. Rev.* **65**, 117 (1944); C. N. Yang, *Phys. Rev.* **85**, 808 (1952).

⁴L. D. Roelofs, A. R. Kortan, T. L. Einstein, and R. L. Park, *Phys. Rev. Lett.* **46**, 1465 (1981).

⁵I. F. Lyuksyutov and A. G. Fedorus, *Zh. Eksp. Teor. Fiz.* **80**, 2511 (1981) [*Sov. Phys.—JETP* **53**, 1317 (1981)].

⁶C. C. Chang and L. H. Germer, *Surf. Sci.* **8**, 115 (1967).

⁷J. C. Tracy and J. M. Blakely, *Surf. Sci.* **15**, 257 (1969).

⁸H. L. Davis and G.-C. Wang, *Bull. Am. Phys. Soc.* **29**, 221 (1984). The $p(2 \times 1)$ -O overlayer does not cause the tungsten substrate to reconstruct, but introduces a reduction of both lateral and vertical relaxation. The oxygen atoms are most like-

ly to sit at the position shown as the hatched circles in Fig. 1(b) from a preliminary dynamical LEED calculation. The exact vertical spacing between the oxygen overlayer and tungsten substrate is yet to be determined.

⁹G.-C. Wang and T.-M. Lu, *Phys. Rev. B* **28**, 6795 (1983).

¹⁰G.-C. Wang and T.-M. Lu, *Phys. Rev. Lett.* **50**, 2014 (1983).

¹¹T.-M. Lu, in *Ordering in Two Dimensions*, edited by S. K. Sinha (Elsevier/North-Holland, Amsterdam, 1980).

¹²J. M. Pimbley, T.-M. Lu, and G.-C. Wang, *Surf. Sci. Lett.* (to be published).

¹³P. M. Horn, R. J. Birgenau, P. Heiney, and E. M. Hammonds, *Phys. Rev. Lett.* **41**, 961 (1978).

¹⁴A. Z. Patashinskii and V. L. Pokrovskii, *The Fluctuation Theory of Phase Transitions* (Pergamon, Oxford, 1979).

¹⁵P. A. Bennett and M. B. Webb, *Surf. Sci.* **104**, 74 (1981).

¹⁶M. Henzler, *Appl. Surf. Sci.* **11/12**, 450 (1982).

¹⁷J. A. Martin and M. G. Lagally, *J. Vac. Sci. Technol.* **A1**, 1210 (1983).